Journal of Chromatography A, 1225 (2012) 158–167

Contents lists available at SciVerse ScienceDirect

Journal of Chromatography A

journal homepage: www.elsevier.com/locate/chroma

Novel peptide ligand with high binding capacity for antibody purification

Line Naomi Lund[a,e,*], Per-Erik Gustavsson[a], Roice Michael[a], Johan Lindgren[b], Leif Nørskov-Lauritsen[a], Martin Lund[c], Gunnar Houen[d,e], Arne Staby[a,f], Phaedria M. St. Hilaire[a]

[a] Novo Nordisk A/S, Hagedornsvej 1, DK-2820 Gentofte, Denmark
[b] Bio-Works Sweden AB, Annedalsvägen 39, 16865 Bromma, Sweden
[c] FeF Chemicals A/S, Københavnsvej 216, DK-4600 Køge, Denmark
[d] Department of Clinical Biochemistry and Immunology, Statens Serum Institut, Artillerivej 5, DK-2300 Copenhagen, Denmark
[e] Department of Biochemistry and Molecular Biology, University of Southern Denmark, Campusvej 55, DK-5230 Odense M, Denmark
[f] Department of Chemical Engineering, Lund University, 22100 Lund, Sweden

ARTICLE INFO

Article history:
Received 17 August 2011
Received in revised form
15 December 2011
Accepted 23 December 2011
Available online 29 December 2011

Keywords:
Small synthetic peptide ligands
Mixed-mode chromatography
Monoclonal antibody purification
Isothermal titration calorimetry
High throughput screening

ABSTRACT

Small synthetic ligands for protein purification have become increasingly interesting with the growing need for cheap chromatographic materials for protein purification and especially for the purification of monoclonal antibodies (mAbs). Today, Protein A-based chromatographic resins are the most commonly used capture step in mAb down stream processing; however, the use of Protein A chromatography is less attractive due to toxic ligand leakage as well as high cost. Whether used as an alternative to the Protein A chromatographic media or as a subsequent polishing step, small synthetic peptide ligands have an advantage over biological ligands; they are cheaper to produce, ligand leakage by enzymatic degradation is either eliminated or significantly reduced, and they can in general better withstand cleaning in place (CIP) conditions such as 0.1 M NaOH. Here, we present a novel synthetic peptide ligand for purification of human IgG. Immobilized on WorkBeads, an agarose-based base matrix from Bio-Works, the ligand has a dynamic binding capacity of up to 48 mg/mL and purifies IgG from harvest cell culture fluid with purities and recovery of >93%. The binding affinity is $\sim 10^5\ M^{-1}$ and the interaction is favorable and entropy-driven with an enthalpy penalty. Our results show that the binding of the Fc fragment of IgG is mediated by hydrophobic interactions and that elution at low pH is most likely due to electrostatic repulsion. Furthermore, we have separated aggregated IgG from non-aggregated IgG, indicating that the ligand could be used both as a primary purification step of IgG as well as a subsequent polishing step.

1. Introduction

Small synthetic ligands for protein purification have become increasingly interesting with the growing need for cheap chromatographic materials for protein purification and especially for the purification of monoclonal antibodies (mAbs) [1–3]. Today, Protein A-based chromatographic resins are the most commonly used capture step in mAb down stream processing; however, the use of Protein A chromatography is less attractive due to toxic ligand leakage [4–7] as well as high cost [8]. Different chromatographic alternatives for mAb purification have been widely investigated and comprise as diverse molecules as dyes [9–11], Protein A mimetic ligands [3,12–14], mixed-mode ligands [2,15] and other small synthetic ligands [16,17]. Unfortunately, these small synthetic ligands have had limited commercial success due to poor overall performance compared to, e.g. MabSelect SuRe (GE Healthcare). However, recently attention has been drawn to the ability of these chromatographic resins to remove antibody aggregates [18–21], host cell protein (HCP) impurities [22–24] as well as leaked Protein A from the capture step [24]. Hence, the small peptide ligands could be used as a polishing step in either capture or flow through mode [22,23]. Whether used as an alternative to the Protein A chromatographic media or as a subsequent polishing step, small synthetic peptide ligands have an advantage over biological ligands; they are cheaper to produce, ligand leakage by enzymatic degradation is either eliminated or significantly reduced, and they can in general better withstand cleaning in place (CIP) conditions such as 0.1 M NaOH. The latter two qualities give the synthetic peptide ligand resins a longer lifetime, since the resins do not suffer from loss of binding capacity. Furthermore, the generic mAb purification platforms developed by the biopharmaceutical

* Corresponding author at: Novo Nordisk A/S, Brudelysvej 22, DK-2880 Bagsværd, Denmark. Tel.: +45 4444 8888.
E-mail address: LNmL@novonordisk.com (L.N. Lund).

0021-9673/$ – see front matter © 2012 Elsevier B.V. All rights reserved.
doi:10.1016/j.chroma.2011.12.074

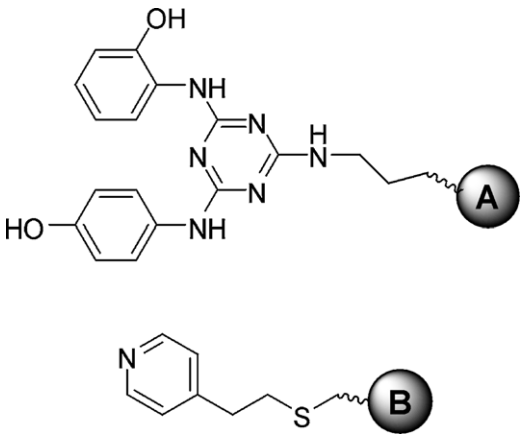

Fig. 1. The structure of the two commercially available small ligands, A2P (A) and MEP (B), used for IgG purification.

industry are generally efficient and replacing, e.g. a commonly used step such as Protein A-chromatography with a less well studied small ligand-based resin can be expensive. Such a replacement requires convincing business cases as well as thorough process studies.

Two peptide ligands that have managed to stay on the market are MABsorbent A2P (Prometic Biosciences) and MEP HyperCel (Pall), both presented in Fig. 1; the two ligands have previously been compared with respect to using IgG1, IgG2, and Fc1 fusion proteins to characterize their performance [25]. MABsorbent A2P is a Protein A-mimetic affinity ligand based on the dye trichlorotriazine and coupled to a 6% cross-linked agarose chromatographic resin (PuraBead 6XL) capable of withstanding high flow rates [25,26]. Furthermore, the resin can purify polyclonal antibodies as it does not distinguish between Ig isotypes [27–29]. MEP HyperCel, currently denoted as a mixed-mode resin, was originally presented as hydrophobic charge induction chromatographic (HCIC). The ligand shown in Fig. 1 was selected from a group of amine, carboxylic acid or thiol based ligands [30]; however, the 4-mercapto-ethylpyridine (MEP) ligand proved to purify mAb efficiently though with some non-specific interactions with HCP [15,25].

Here, we present two novel synthetic peptide ligands, D_2AAG and DAAG, with mixed-mode characteristics for mAb purification. The ligands were identified by combinatorial library screening [31] and further structural design hereof. Both ligands contain natural amino acids, L-arginine and L-glycine, as well as a synthetic, aromatic acid, 2,6-di-t-butyl-4-hydroxybenzyl acrylate (DBHBA), as shown in Fig. 2. We tested the effect of different chromatographic media as well as the interaction with various mAbs. The dynamic binding capacity at 10% breakthrough (10% DBC), purity and recovery were measured and benchmarked against the industry standard, MabSelect SuRe, as well as a few small ligand-based chromatographic media. Moreover, the ligand-mAb interaction was investigated using isothermal titration calorimetry (ITC) providing thermodynamic parameters. The calorimetric and chromatographic results were compared with static and dynamic high throughput experiments (HTE), evaluating possible differences between free ligand behavior and immobilized ligand behavior.

2. Materials and methods

2.1. Materials

2.1.1. Monoclonal antibodies

Five in-house mAbs of immunoglobulin isotype 4 (IgG4) designated IgG4-A to IgG4-E and two in-house IgG1 antibodies named

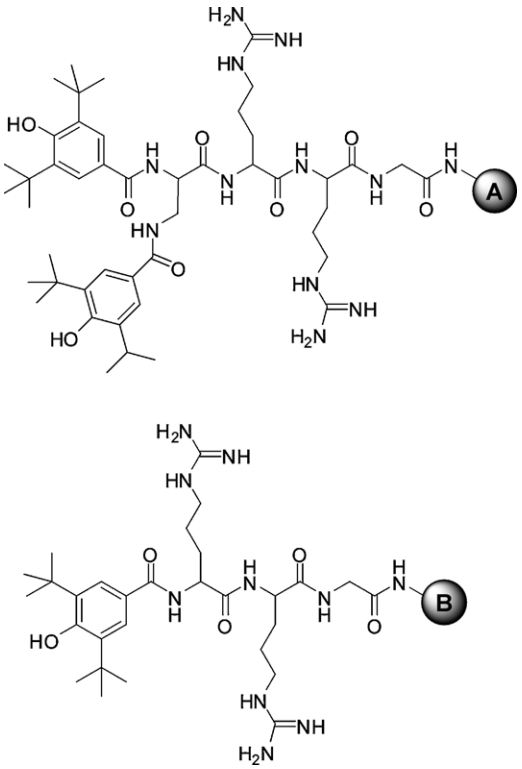

Fig. 2. The structure of the two novel synthetic peptide-based ligands D_2AAG (A) and DAAG (B).

IgG1-A and IgG1-B were used. Furthermore, we have investigated binding to Fc fragments of IgG4-A and IgG1-A called Fc-4 and Fc-1, respectively, and an in-house F(ab′)$_2$ fragment.

Antibody aggregates were deliberately induced after purification on Protein A resin by lowering the pH to 3.4 for 60 min at room temperature in aliquots of 10 mL under slow agitation followed by readjustment to pH 5. The samples were analyzed by SEC and the amount of aggregates determined from the UV absorbance at 280 nm.

2.1.2. Chemicals

The reagents for all solvents were purchased from Merck KGaA (Darmstadt, Germany).

2.1.3. Chromatographic media

The following chromatographic base media were purchased or kindly provided by the manufacturers: WorkBeads™ (Bio-Works AB, Bromma, Sweden); Amino Sepharose 6FF (GE Healthcare, Uppsala, Sweden); Cellufine Amino (Chisso, Tokyo, Japan) and Toyo Pearl AF 650S (Tosoh Biosciences, Tokyo, Japan). Furthermore, the following resins were purchased or kindly provided by the manufacturers: 6% Rapid Run (ABT Agarose Bead Technology, Madrid, Spain); MEP HyperCel (Pall, Port Washington, NY, USA); MABsorbent A2P (Prometic Biosciences, Cambridge, UK); MabDirect MM (Up-Front, Copenhagen, Denmark) and MabSelect SuRe, Protein A Sepharose and Protein G Sepharose (GE Healthcare).

2.1.4. Ligand synthesis

The synthetic peptide ligands D_2AAG and DAAG were synthesized as previously described [31].

2.2. Methods

2.2.1. Chromatographic evaluation on Äkta Explore 100

The column chromatographic experiments were performed using Fast Protein Liquid Chromatographic system (Äkta Explorer

100; GE Healthcare) system equipped with a 50 mL superloop, 2-mm UV flow cell and a Fraction-950. Tricorn 5/100 columns (GE Healthcare) were packed with ~1 mL chromatographic media. All media were tested at a flow rate of 0.33 mL/min (101 cm/h). In all cases eluted fractions were adjusted to pH 7 by 0.5 M sodium diphosphate if necessary and analyzed either by HPLC or on the Bioanalyzer as described in Section 2.2.5. This setup was used for the base resin evaluation with D_2AAG and DAAG, respectively, as well as the binding capacity analysis of IgG4-B, IgG4-C, IgG4-D, IgG4-E, IgG-4F, IgG-1A and IgG1-B reported in Section 3.2. The binding capacity studies were performed using cell culture fluid.

Evaluation of D_2AAG and DAAG coupled to various base resins were tested using the following setup on the Äkta: After a 15 CV pre-wash with 50 M sodium phosphate 100 mM sodium chloride pH 7 (wash buffer), the sample (15–20 mg IgG) was loaded using the superloop. The column was then washed with 15 CV wash buffer and eluted with 25 CV 10 mM sodium formate, 100 mM sodium chloride pH 3.6. The column was regenerated first by 5 CV of wash buffer, followed by 5 CV of 0.5 mM sodium hydroxide and re-equilibrated with 10 CV of wash buffer.

Mabsorbent A2P was analyzed as follows: After a pre-wash with 15 CV of 25 mM sodium phosphate 100 mM sodium chloride pH 7.5 (wash buffer), the sample (20 mg IgG) was loaded from the superloop, followed by a 15 CV wash with the wash buffer and elution by 25 CV of 50 mM sodium citrate pH 3 and 5 CV 50 mM sodium citrate pH 2. The column was regenerated as described above.

MEP HyperCel was tested using the following protocol: the sample (40 mg IgG) was loaded using the superloop after a 15 CV pre-wash with 50 mM Tris–HCl pH 7.5 (wash buffer). Then followed by a 15 CV wash with the wash buffer and elution with 25 CV 100 mM sodium acetate, 50 mM sodium chloride, pH 3. The column was then regenerated as described above.

MabDirect followed this protocol: After a 15 CV pre-wash with 20 mM sodium citrate, 100 mM sodium chloride, pH 5.6, the sample (20 mg IgG) was loaded, followed by a 15 CV wash with the wash buffer. Elution was done with first 25 CV of 100 mM Tris–HCl, 100 mM sodium chloride, pH 8.2 and 25 CV 100 mM Tris–HCl, 500 mM sodium chloride, pH 5.6. The resin was regenerated as described above.

MabSelect SuRe, Protein A Sepharose and Protein G Sepharose were all tested according to the following scheme: A 15 CV pre-wash with 50 M sodium phosphate, 300 mM sodium chloride, pH 7 (wash buffer), the sample (25 mg IgG) was loaded using the superloop. The columns were then washed with 15 CV wash buffer and eluted with 25 CV 10 mM sodium formate, pH 3.6. Columns were regenerated as described above.

2.2.2. Chromatographic evaluation on HTE system

The 200 μL MediaScout RoboColumns (Atoll GmbH, Weingarten, Germany) were used for chromatographic screening on a Tecan Evo Freedom 200 (Tecan, Crailsheim, Germany) equipped with two liquid handling arms and one gripper, a centrifuge (Rotanta 46 RSC, Hettich, Tuttlingen, Germany) and an 2104 EnVison Multilabel Reader (PerkinElmer, Skovlunde, Denmark). The Tecan robots were controlled by the software package Evoware 1.4 while the photometer was controlled by Magellan 6.0 (Tecan, Crailsheim, Germany). The buffers used for the chromatographic tests are described in details in Section 2.2.1. A flow rate of 0.3 mL/min was used for all steps; furthermore, all columns were pre-washed with the appropriate buffer 6 CV, followed by loading of 5.5 mg IgG4-B. The columns were then washed with 6 CV of the appropriate buffer collected in three 96-well plates before elution with 8CV of the appropriate elution buffer and regeneration.

2.2.3. Aggregate removal

Aggregate removal was investigated using pre-purified IgG4-E (50 mg) with >10% aggregates loaded on 1 mL DAAG-WorkBead column. The column was then run as described in Section 2.2.2. The eluted fractions were analyzed for aggregates on a TSK Gel G3000 SWXL column from Tosoh Biosciences (Tokyo, Japan).

2.2.4. $F(ab')_2$ and Fc fragment binding

The Äkta system setup and the buffer systems described in Section 2.2.1 were applied to the appropriate chromatographic resins in a competitive binding study where an artificial mixture or Fc-4 and $F(ab')_2$ fragment was loaded. The amount of Fc-4 fragment loaded was the same as the amount of IgG-4A, as stated in Section 2.2.1, while the amount of $F(ab')_2$ fragment was 75% of the amount of Fc fragment (w:w).

2.2.5. Isothermal titration calorimetry

All proteins were dialyzed using Slide-A-Lyzer, 10000 MWCO, 0.5–3 mL (Pierce Biotechnology, Rockford, IL, USA) into 50 mM sodium phosphate buffer, augmented with 100 mM sodium chloride, pH 7 overnight at 5 °C. Protein concentration was determined using UV absorbance at 280 nm on a NanoDrop ND-1000 spectrophotometer (NanoDrop Technologies, Wilmington, DE, USA) using the molar extinction coefficients: 2.1×10^5 for IgG-4A and 7.0×10^4 for Fc-4. $F(ab')_2$ concentration was measured on the Bioanalyzer 2100 (Agilent Technologies, Santa Clara, CA, USA).

The titration experiments were carried out on a VP-ITC (MicroCal™, Piscataway, NJ, USA) at 25 °C. A 250 μL syringe was used for the ITC injections at a stirring speed of 210–307 rpm. The first injection was 2 μL and subsequent injections were of a volume of 10–13 μL every 5 min. In all experiments, the IgG-binding protein was injected into the cell containing IgG-4A or Fc-4. Concentrations of D_2AAG-3PEG and DAAG-3PEG in the syringe ranged from 0.8 to 1.3 mM while IgG-4A or Fc-4 fragment concentrations in the cell were between 0.2 and 0.6 mM. All samples were degassed for 10 min prior to the experiment and all experiments were done in triplicates. The results were analyzed with Origin 7, MicroCal LLC ITC and fitted to a single site model. In this way, the stoichiometry (n), the thermodynamic association constant (K_a) and enthalpy change (ΔH°) can be calculated directly. The Gibbs free energy change (ΔG°) was calculated from the equation: $\Delta G^\circ = -RT \ln K_a$, where R is the molar gas constant and T the absolute temperature at which the experiment was carried out. The entropy change of the interaction ($T\Delta S^\circ$) was calculated according to the equation: $T\Delta S^\circ = \Delta H^\circ - \Delta G^\circ$.

2.2.6. Adsorption isotherms measurements

The Tecan Evo Freedom 200 (Tecan, Crailsheim, Germany) equipped with two liquid handling arms and one gripper, a centrifuge (Rotanta 46 RSC, Hettich, Kirchlengern, Germany) and an InfiniTe M200 photometer (Tecan) was used. The Tecan robot was controlled by the software package Evoware 1.4 while the photometer was controlled by Magellan (Version 6.0; Tecan). 7 μL resin plugs were transferred to a 1.2 mL deep well plate (DWP). Prior to use, the resin was washed with several portions of the appropriate washing buffer. Eight IgG4-A concentration gradients in duplicates at two different pH values were mixed in an empty 1.2 mL DWP and 500 μL transferred to the resin containing DWP. The resin was incubated with IgG4-A for 120 min at room temperature on a shaker at 900 rpm, followed by centrifugation at 4000 rpm for 5 min. 200 μL of the supernatant was removed and analyzed at 280 nm. The amount of IgG bound (q) was calculated by mass balance and the data fitted to a Langmuir isotherm (1):

$$q = \frac{q_{\max} C}{K_D + C} \quad (1)$$

Table 1
Binding capacity as 10%DBC in mg mAb per mL resin and ligand density in μmol ligand per mL.

Base matrix	Binding capacity (mg/mL)	Ligand density (μmol/mL)	Capacity/density index
D_2AAG			
Sepharose	15	9.3	1.6
Cellufine	12	9.3	1.3
Toyo 650S	15	42.6	0.4
10-PEG Toyo 650S	17	21.7	0.8
DAAG			
Sepharose	24	14.1	1.7
Cellufine	21	41	0.5
Rapid Run	15	19.4	0.8
WB	48	20.3	2.4
Commercial available resins			
MabSelect Sure	32	–	–
A2P	4	20[a]	0.2
MabDirect	10	32	0.3
MEP HyperCel	8	80–125	0.06–0.1

Information kindly provided by Prometic Biosciences.
[a] μmol/g settled gel.

where q_{max} is the maximum binding capacity, C is the concentration and K_D is the dissociation constant.

2.2.7. Ligand docking

Dockings were performed using the computer program GOLD version 5.0.1, available through the Cambridge Crystallographic Datacentre [32]. The protein structure used was 1OQO.pdb from the Protein Data Bank [33] with the Protein A fragment removed.

2.2.8. Sample analysis

Load, flow through, wash, and elution fractions were analyzed either by HPLC or on a Bioanalyzer 2100. A Gilson HPLC system (Middleton, WI, USA) was equipped with a 235 auto-injector, 322 pump-module, and 119 UV/vis detector using a BioSep-SEC-S 3000 size-exclusion chromatography column (Phenomenex, Torrance, CA, USA) and run at 0.8 mL/min. 200 mM sodium phosphate 300 mM sodium chloride 10% isopropanol pH 6.9 was used as the mobile phase and the injected volume was 20, 10 and 5 μL. Analysis on the Bioanalyzer 2100 was performed using the Bioanalyzer Protein 230-kit.

3. Results and discussion

3.1. Chromatographic evaluation of base matrices

We investigated the performance of two small synthetic peptide ligands coupled to different agarose, cellulose and acrylated chromatographic base matrix supports. Fig. 3A and B as well as Table 1 show the binding capacity as 10% DBC, purity and recovery of D_2AAG and DAAG, respectively, for purification of antibody IgG4-B from cell culture harvest. As seen from Fig. 3A and B the overall results combining 10% DBC, purity and recovery shows that the agarose-based media Sepharose FF and the WorkBeads™ from Bio-Works perform best. We found the binding capacity for D_2AAG-Sepharose FF to be 15 mg/L while purity and recovery was found to be 93% and 88%, respectively. For the DAAG ligand the binding capacity on the two resins was found to be 24 mg/mL and 48 mg/mL for Sepharose FF and the BW-resin, respectively, while purity was >93% and recovery was >85% for both resins.

The length of the spacer arm connecting the ligand to the base matrix may influence, e.g. the binding capacity. This was also the result for D_2AAG-10PEG-Toyo Pearl; improved binding capacity and purity was seen but recovery was reduced compared with the results for D_2AAG-Toyo Pearl as seen in Fig. 3A. The enhanced binding capacity is well in line with the improved access to the ligand

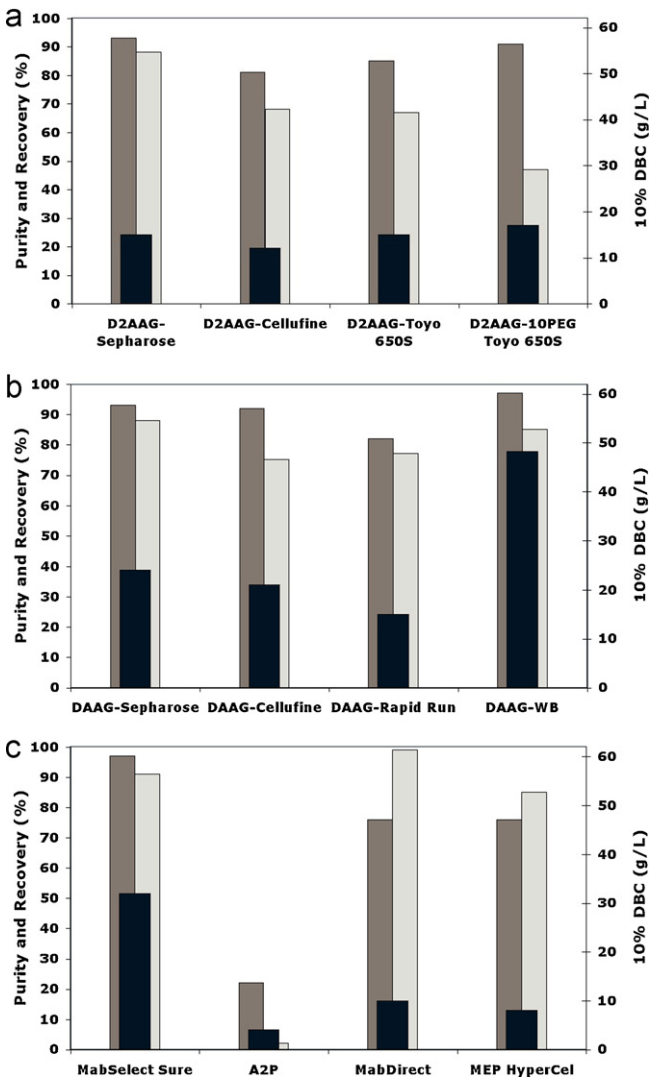

Fig. 3. Chromatographic evaluation of D_2AAG (A) and DAAG (B) on different base resins as well as four commercially available mAb purifying resins (C). 10% DBC (black) is shown in mg/mL while purity (dark grey) and recovery (light grey) in % of total amount loaded on the column. The same mAb was used for all experiments.

due to increase in ligand flexibility and spatial rotation provided by the 10PEG spacer. However, the reduced recovery was unexpected and may be explained by unbound or loosely bound IgG being washed off.

The D_2AAG-Cellufine resin showed the lowest binding capacity of 12 mg/mL while recovery and purity were comparable to those of Toyo Pearl 650S. However, Cellufine showed better results with the DAAG ligand; we found the 10% DBC to be 21 mg/mL. It should be noted that of all the resins investigated, Cellufine had the largest particle size (125–210 μm) while the remaining resins had an average particle size of approximately 100 μm except for WorkBeads (40 μm); larger particle size is know to cause reduced binding capacity [34]. DAAG-Rapid Run gave the lowest binding capacity of 15 mg/mL. This result is most likely explained by the difference in pore size, volume and geometry, which affect the low molecular weight limit (M_{lim}); Rapid Run has a M_{lim} of 1×10^6 while Cellufine has a M_{lim} of 4×10^6. The larger pores of Cellufine most likely result in improved mass transport and hence improved DBC seen for DAAG-Cellufine compared to DAAG-Rapid Run.

The excellent results seen for the D_2AAG and DAAG ligands on Sepharose FF and on the WorkBeads may in part be explained by the resin structure which in both cases is highly cross-linked

agarose. The superior binding capacity on the WorkBeads resin is expected to be because of the highly porous particles allowing a high ligand density due to the increased accessible surface area. We determined the ligand density to be slightly higher in the case of DAAG-WorkBeads as shown in Table 1. However, the ligand density is not twice as high so it appears that the ligands are more easily accessible compared to the ligands of DAAG-Sepharose. Furthermore, we found that the ligand density on the different base resins was not indicative for the 10% DBC. Sepharose FF coupled to either of the two synthetic ligands gave a good capacity/density index; hence the binding capacity was high compared to the ligand density. The same was seen for Cellufine; the ligand density of DAAG-Cellufine is four times higher compared to D_2AAG-Cellufine; however, the binding capacity was only doubled. This phenomenon has previously been noticed and the conclusion by Wrzosek et al. was that the binding capacity reached a maximum at some ligand density on anion exchange resins [35]; at higher ligand densities, the binding capacity would no longer increase and at some point would start to decrease. Pore size and pore geometry may in part account for the observed ligand density optimum. In addition, Brooks and Cramer have found that the increased ligand density on anion exchange resins caused an increase in the amount of sterically shielded ligands. This finding was later confirmed for affinity purification by Ghose et al. who showed that there does not exist a linear relationship between Protein A ligand density and the binding capacity [36]. Considering the cost of ligand production, it may not be desirable to use the ligand density which gives the highest possible binding capacity. However, compared to a biological ligand such as Protein A, which is expressed in bacteria and hence must be purified from crude extract before attachment to the chromatographic resin, small synthetic peptide ligands are considerably cheaper to produce.

For comparison, commercial Protein A ligands and Protein A mimetic ligands were also tested. MabSelect SuRe gave the best overall results with a 10% DBC of 32 mg/mL and purity and recovery above 90% which was expected [37,38]. Surprisingly, MABsorbent A2P showed the poorest ability to purify IgG4-A with negligible recovery and a very low 10% DBC of just 4 mg/mL, which is considerably lower than previous reports of 10.4 mg/mL [39] as well as reports by the manufacturer. Our findings were unexpected as Tugcu et al. presented their results as 1% DBC, which results in lower binding capacities compared to the frequently used 10% DBC [39]. Tugcu et al. does not provide information on the IgG isotype but does list a pI range of 6.1–8.5, within which the pI of our IgG4-B antibody falls. Furthermore, pH of the load is also comparable and moreover, ligand A2P should not be restricted in binding by Ig isotype. However, our media contains Phenol Red which can cause reduced binding of IgG according to the manufacture. They recommend an initial purification step on an ionexchange resin. However, while this may solve the problem with loss of binding capacity on the A2P resin, it results in more work and hence, a less quick purification process. For this reason, we have not investigated if removal of Phenol Red would increase the binding capacity on MABsorbent A2P.

HEP HyperCel also showed a surprisingly low binding capacity while purity and recovery were good. These results were, however, more in line with the findings of Tugcu et al. [39]. MabDirect from Up-Front gave high recovery and good purity while the binding capacity was in the lower end with just 10 mg/mL.

Systematic screening of ligands and base resins can be time consuming primarily because of the time spent coupling the ligands to the base resin and partly because of the time spent performing the analysis on the Äkta system. Therefore, we performed the resin analysis using a Tecan robot system on which we measured the 10% DBC on a 200 μL scale, running eight RoboColumns in a single 3-h experiment. As seen from Table 2, the 10% DBC obtained on the 200 μL scale is generally in good agreement with the capacities found on the 1 mL scale. However, in the case of MEP HyperCel we found that the binding capacity on the 200 μL scale was three times higher compared to the 1 mL scale. In addition, the 200 μL scale results are higher than those found by Tugcu et al. [39]; a possible explanation may be in the way that the RoboColumns were packed though we saw similar results for other resins packed in RoboColumns. However, we can now in a very short time obtain multiple results on binding capacity by varying, e.g. loading pH or the buffer system in order to select the best resin and the appropriate buffer system.

Table 2
10%DBC in mg mAb per mL resin measured on 1 mL resin columns tested on Äkta Explorer and 200 μL resin RoboColumns tested on Tecan Evo robot.

Base matrix	10% DBC – 1 mL (mg/mL)	10% DBC – 200 μL (mg/mL)
DAAG-Sepharose	24	22.8 ± 2.6
D_2AAG-Sepharose	15	15.1 ± 2.0
MabSS	32	35.8 ± 1.6
MEP HyperCel	8	26.8 ± 2.6
Protein A Sepharose	20[a]	31.7 ± 1.5
Protein G Sepharose	30[a]	22.5 ± 2.0

[a] Binding capacity data provided by GE Healthcare.

3.2. Evaluation of mAb pI binding capacity dependence

We have tested several in-house mAbs with different pI values on D_2AAG- and DAAG-Sepharose and DAAG-WorkBeads. As seen from Fig. 4, the three resins display different capacities for antibodies of the same isotype but with different pI values. Moreover, no apparent correlation is obtained between antibody pI and the binding capacity. Our results may have different explanations: Ghose et al. have shown that different IgG1 antibodies and Fc fusion proteins with identical Fc fragments, does not show the same binding capacity on Protein A chromatographic media [36]. While they did not relate the binding capacity to the pI value, they concluded that the apparent size and shape, though not the molecular weight of the proteins influenced binding. This may also explain our results; an overlay of the different IgG4 molecules shows that there are only structural differences in the Fab arms (purple parts in Fig. 5). Hence, the shape of the Fab arms may very well differ and could cause the difference in binding capacity that we experience. The results also provide information on the interaction between the ligands and the IgGs. If the binding resulted primarily from ionic interactions, we would expect to obtain a pI dependency of the binding capacity. Since this is not the case, it is likely that hydrophobic forces dominate the interaction.

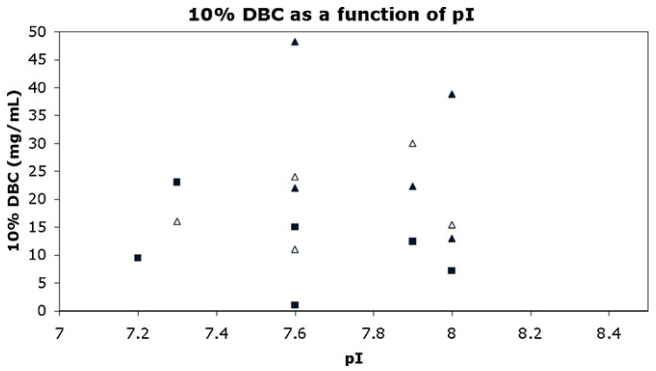

Fig. 4. 10% DBC shown in mg/mL as a function of mAb pI. Black squares represent D_2AAG-Sepharose, open triangles represent DAAG-Sepharose and black triangles DAAG-BW.

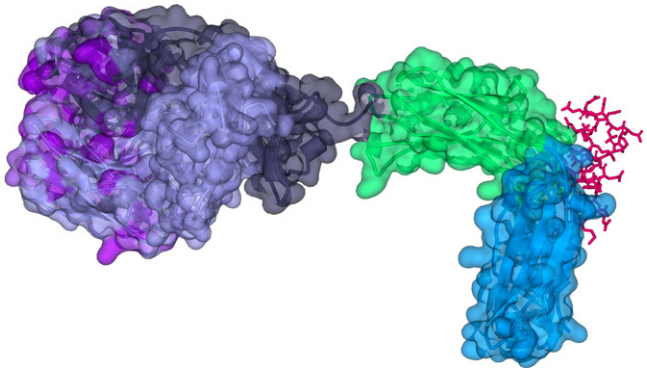

Fig. 5. Overlay showing half structures of IgG4-B, IgG4-C, IgG4D and IgG4E. The blue and green colour represents the CH2 and CH3 domain of the Fc fragments, while the grey colour represents the Fab-arm. The purple parts indicate structural differences between the four antibodies. The red stick structure shows the Protein A binding site. (For interpretation of the references to color in this figure legend, the reader is referred to the web version of this article.)

3.3. Immunoglobulin G fragment binding

Due to the results presented in Section 3.2, we decided to perform a competitive study to determine the degree of ligand binding to the Fab arms. This was done by loading a mixture of equal amounts (mg) of Fc fragment and $F(ab')_2$ fragment as shown in Fig. 6. The DAAG-ligand coupled to Sepharose FF showed a low capacity for $F(ab')_2$ fragment, binding only 6% of the applied amount. In addition, the ligand bound 71% of the applied Fc fragment; an overall good performance compared to the MABsorbent A2P, MEP HyperCel, and MabDirect: MABsorbent A2P bound 87% of the applied $F(ab')_2$ fragment and only 62% of the applied Fc fragment. Since the A2P ligand was designed to mimic the binding of Protein A, we did not expect this outcome. Furthermore, MabDirect and MEP HyperCel bound all applied $F(ab')_2$ fragment while only ~20% of the Fc fragment. As expected, MabSelect SuRe did not bind the $F(ab')_2$ fragment.

The results confirm our assumption that the binding between the ligands and IgG is through the Fc fragment. Moreover, our results are well in line with the calorimetric results presented in Section 3.5.

3.4. Immunoglobulin aggregate removal

Synthetic mixed-mode ligands have previously been shown to have the ability to separate IgG4 aggregates from IgG monomers and hence, to function as a polishing step after the initial affinity purification on a Protein A-based chromatographic resin [21].

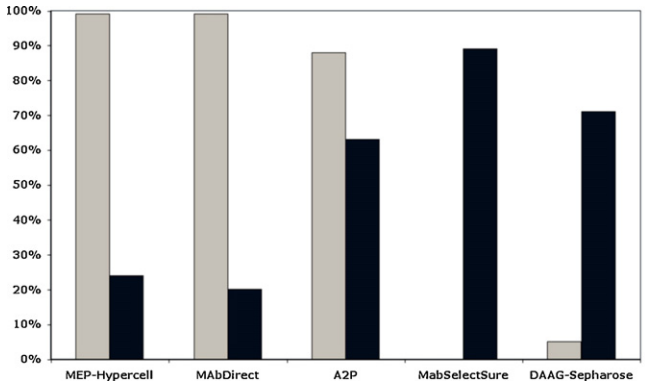

Fig. 6. Binding to four selected commercial available resins and DAAG-Sepharose of Fab (grey) and Fc (black) in competition.

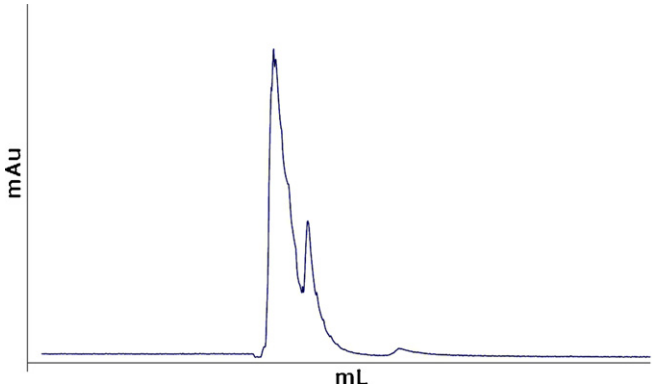

Fig. 7. Aggregate separation on DAAG-WB on a 1 mL column. Pre-purified IgG with more than 10% aggregated IgG was loaded and the monomer-containing peak is clearly separated from the tailing aggregate-containing peak.

We have tested this ability on the DAAG-WorkBead resin to give a complete picture of the resin's purification capability; as seen from Fig. 7, two peaks were separated after loading a pre-purified IgG4 with a high content of aggregates (>10%). The first peak seen on the chromatogram proved to be IgG monomer, while the tailing peak contained aggregates of different size as determined by size exclusion chromatography. Previously, separation of IgG aggregates from monomers has been suggested on MEP HyperCel [19]; however no experimental data has been published. It should be noted that binding, washing, or elution conditions were not optimized for the separation of IgG aggregates. Hence, it is likely that an elution gradient would improve the elution profile compared to the isocratic elution used herein and this subject will be investigated further.

3.5. Thermodynamic analysis and association constant determination

Thermodynamic analysis of the interaction between IgG4, Fc4, or $F(ab')_2$ fragment and D_2AAG was conducted using ITC; our results revealed that interaction between IgG4-A and D_2AAG was located at the Fc fragment, supporting our previous findings presented in Section 3.3. The thermodynamic data was calculated per binding site; a thermogram of the titration of IgG4-A with D_2AAG is shown in Fig. 8. Interestingly, the K_a values for the binding of IgG4-A and Fc4 were the same and so were the remaining thermodynamic parameters as seen in Table 3. However, the stoichiometries, N, were different; while only a single molecule of IgG4-A was bound by D_2AAG, the ligand bound two molecules of Fc4. Hence, we find that the presence of the $F(ab')_2$ fragment on IgG does influence the interaction between protein and ligand though it does not change the strength or the nature of the interaction. The interaction between D_2AAG and IgG4-A or Fc4 is favorable as seen from the large and negative Gibbs free energy; moreover, the binding of IgG4 or Fc4 is entropically driven. It has previously been shown, that hydrophobic interactions are associated with a favorable change in entropy [40,41] while ionic interactions are dominated by favorable changes in the enthalpy [41,42]. Hence, the results of D_2AAG points to that the binding of the Fc fragment of IgG is mediated by hydrophobic interactions. However, it is important to keep in mind that conformational changes also contribute to the thermodynamics of binding.

Similar results were previously presented for the D-form of the PAM (TG19318) ligand once manufactured by Tecnogen (CE, Italy) [12], which is shown in Fig. 9.

The PAM ligand can purify IgG from a wide range of sources as well as other immunoglobulin isotypes such as IgA and IgM [12].

Table 3
Thermodynamic data from ITC experiments in which ligand D_2AAG was titrated into IgG4 or Fc4, respectively.

	K (M^{-1})	ΔH° (kJ/mol)	$T\Delta S^\circ$ (kJ/mol)	ΔG° (kJ/mol)	N
IgG4-A	$7.4 \pm 0.9 \times 10^4$	2.3 ± 0.3	30.1 ± 0.4	−27.8 ± 0.3	0.84
Fc4	$7.9 \pm 1.2 \times 10^4$	1.0 ± 0.02	29.0 ± 0.4	−28.0 ± 0.4	1.96
$F(ab')_2$	N.B.D.	–	–	–	–

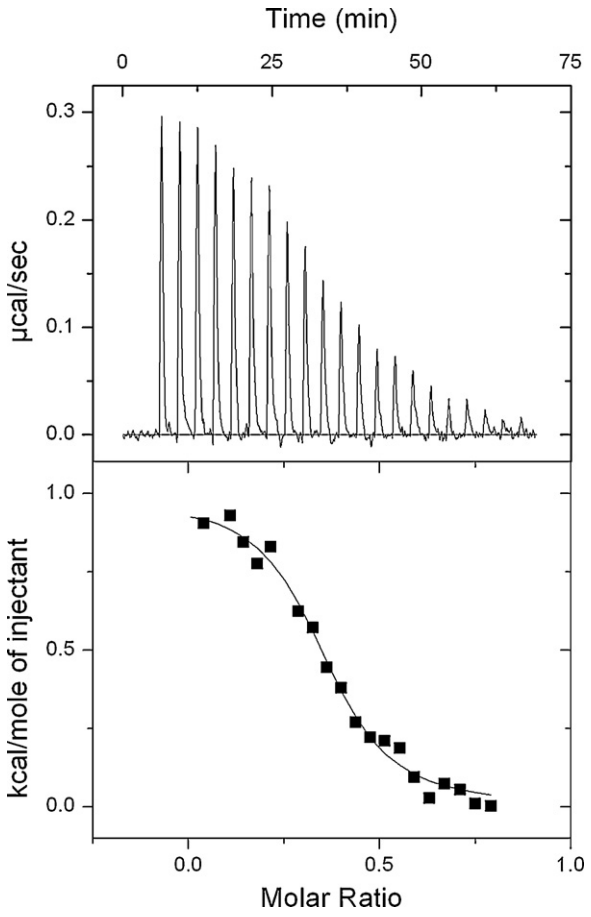

Fig. 8. An ITC thermogram (top) and binding isotherm (bottom) for the interaction between D_2AAG and IgG4. The experiment was performed at 25 °C in 50 mM sodium phosphate, 100 mM NaCl pH 7 with 13 μL injections.

The thermodynamic investigation of the D-form of the PAM ligand (D-PAM) showed that the interaction between D-PAM and IgG was favorable ($\Delta G^\circ = -25.9$ kJ/mol) but unlike the D_2AAG ligand, the interaction with IgG was both enthalpically ($\Delta H^\circ = -5.4$ kJ/mol) and entropically driven ($T\Delta S^\circ = 31.3$ kJ/mol) [14]. Since ΔG° was similar to our findings for D_2AAG, the K_a value (3.4×10^4 M^{-1}) also resembles what we found. However, the stoichiometry showed that

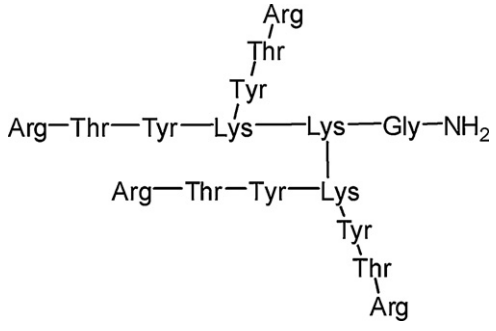

Fig. 9. Structure of the Protein A-mimetic ligand, PAM.

to each IgG molecule two molecules of D-PAM bound; this result is different from our findings of a 1:1 interaction between D_2AAG and IgG4-A. We cannot rule out a concentration-dependent stoichiometric behavior of either ligands as previously seen for Protein A [43,44]; this would require further experiments where the concentration of either the ligand or IgG would vary, however, this is outside the scope of this paper.

While ITC provides information on the free ligand interaction with the antibodies, the K_a value can be obtained by static adsorption at different protein concentrations enabling a binding isotherm deduction. We conducted the static adsorption experiments on a Tecan Evo robot in a HTE setup and tested the binding of IgG4-A at pH 5.2, 6.2 and 7. As seen from Fig. 10, pH of the binding buffer influences the binding of IgG4-A. In the case of D_2AAG-Sepharose, binding at pH 7 ($q_{max} = 43.8$ mg/mL; $K_a = 3.8 \times 10^6$ M^{-1}) was different from binding at pH 6.2 ($q_{max} = 30.5$ mg/mL; $K_a = 4.9 \times 10^5$ M^{-1}) and pH 5.2 ($q_{max} = 20.9$ mg/mL; $K_a = 1.2 \times 10^6$ M^{-1}). Hence, the binding capacity at pH 7 is twice the capacity at pH 5.2 and 50% higher than that at pH 6.2. The strength of binding is also influenced by pH; once more, binding at pH 7 is most favorable, while binding at pH 6.2 appeared to be the least favorable. Interestingly, we found that DAAG-Sepharose did not show the same pH dependency regarding the adsorption constant (pH 7: 6.2×10^6 M^{-1}; pH 5.2: 5.8×10^5 M^{-1}). As seen from Fig. 10B, the slopes at the lower concentrations are similar for the two pH; hence, the K_a values would be similar. However, the maximum binding capacity was influenced significantly by pH; At pH 7 q_{max} was found to be 49.7 mg/mL while it was determined to be 33.4 mg/mL at pH 5.2. This result resembles that found for D_2AAG-Sepharose and may not be surprising as the two ligands are structurally alike; hence, the interaction with IgG is likely to be similar and therefore influenced in the same manner by pH. Surprisingly, DAAG-WorkBeads did not show the expected high maximum binding capacity (~35 mg/mL at pH 7) as previously seen (Section 3.1); however, the association constant was similar to those found for DAAG-Sepharose (pH 7: 1.1×10^6 M^{-1}; pH 6.2: 6.5×10^5 M^{-1}). Hence, our results show that both ligands are highly influenced by pH.

For the D_2AAG and DAAG ligands coupled to Sepharose FF, the K_a values obtained from the binding isotherms as presented in Table 4 were higher than those obtained from ITC (Table 3); in the case of D_2AAG the binding strength was a factor 10 higher. As expected, the q_{max} value was higher than the dynamic binding capacity presented in Section 3.1; more precisely, q_{max} was twice as high as the 10% DBC. The opposite was found for the DAAG ligand on WorkBead. Here, we found that the maximum binding capacity was considerably lower than what was found in the dynamic setup. This result is surprising since we have seen excellent 10% DBC values in

Table 4
q_{max} and K_a from static adsorption experiments performed on Tecan Evo robot.

Resin	q_{max} (mg/mL)	K_a (M^{-1})
Protein A-Sepharose 6FF	29.2	5.7×10^6
Protein G-Sepharose 4FF	18.9	4.5×10^6
MabSelect SuRe	49.8	4.5×10^9
MEP HyperCel	33.3	2.1×10^6
D2-Sepharose 6FF	36.2	7.9×10^5
DAAG-Sepharose 6FF	49.6	2.6×10^6
DAAG-WorkBead	17.7	1.1×10^6

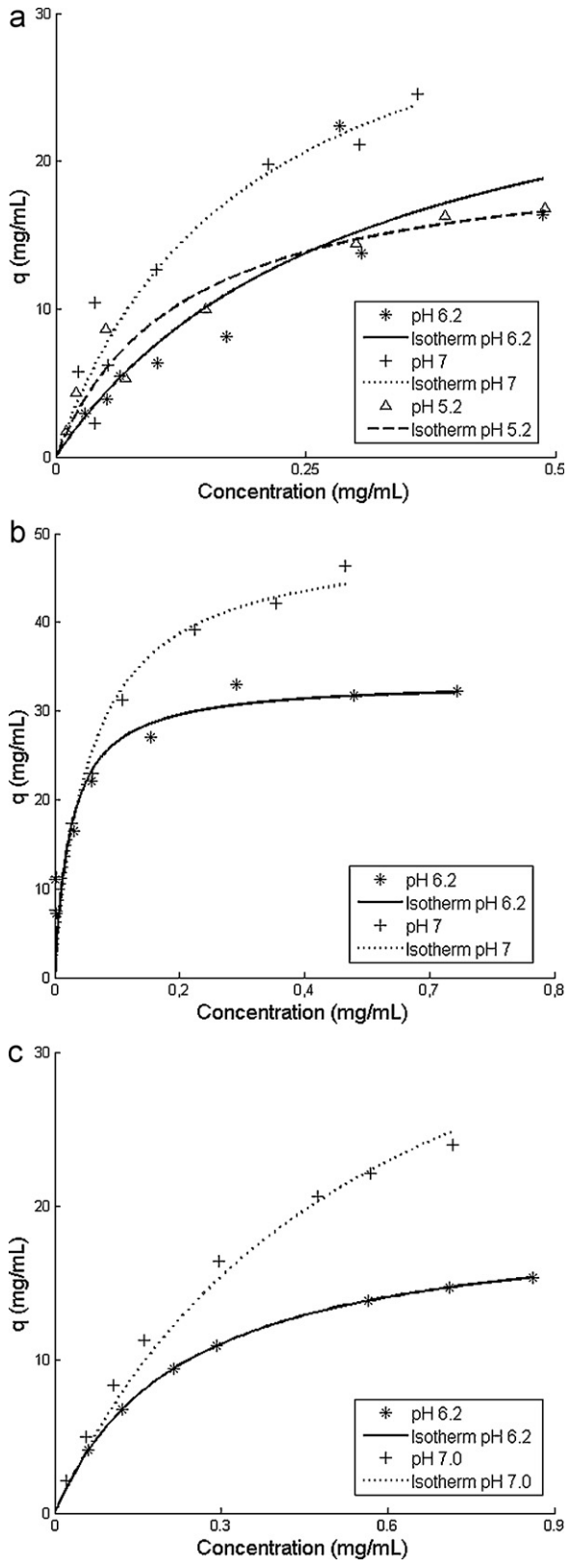

Fig. 10. Batch adsorption of IgG4 on D2AAG- (A) and DAAG-Sepharose (B) and DAAG-WB (C) at different pH 5.2, 6.2 and 7.0. The data points are shown as (+ or *) while the calculated Langmuirian isotherms are shown as lines.

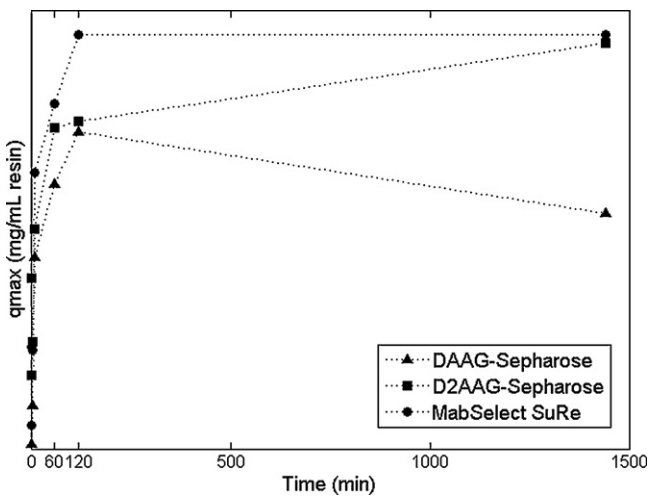

Fig. 11. q_{max} as a function of incubation time when determining q_{max} and K_a values during batch adsorption for three resins at pH 7.

multiple runs with the resin. Based on the small particle size of the WorkBeads, we would expect that 2 h incubation would have been sufficient to reach q_{max}. Furthermore, we found that q_{max} for Protein A Sepharose was half of what has previously been reported by Hahn et al., determined by dynamic breakthrough curves at different IgG concentration using 0.5 mL resin in each column [45]. They found the maximum binding capacity to be 61.6 mg/mL and K_a to be $0.25 \times 10^6\ M^{-1}$, the latter of which is well in line with our findings. Interestingly, we have previously investigated the interaction between IgG4-A and Protein A or Protein G from GE Healthcare by ITC and then determined a K_a of $1.0 \times 10^8\ M^{-1}$ and $1.2 \times 10^8\ M^{-1}$, respectively [2170; these K_a values are a factor 10^3 higher than the batch adsorption results (Table 4). Furthermore, the subsequent findings for MabSelect SuRe by Hahn et al. were also high compared to our findings; they calculated q_{max} to be 61.2 mg/mL while K_a was found to be $7.7 \times 10^6\ M^{-1}$ [37]. In comparison, our investigation using free MabSelect SuRe ligand by ITC indicated a $K_a > 10^9\ M^{-1}$ (the limit of the ITC apparatus) [44]. In addition, Ghose et al. have previously analyzed MEP HyperCel by batch adsorption on a 1 mL scale incubated for 24 h and found it to be $1.35 \times 10^5\ M^{-1}$ [25]. The K_a value calculated by us using batch adsorption is a factor 10^2 higher. Hence, it is difficult to obtain comparable results using different experimental setups and this must be taken into account when acquiring thermodynamic data.

The error of the absolute values for the maximum binding capacity could potentially be large due to the small amount of resin used in the HTE setup; however, Herrmann et al. have previously shown that the plaques are produced with >98% accuracy [46]. We have not tested the accuracy of our setup and hence, cannot rule out errors due to the plaque casting technique. Furthermore, Ma et al. have calculated the inter-day and intra-day accuracy of a Tecan Evo equipment similar to the one used herein and found those to be <7.2% and <5.3%, respectively. Hence, system errors do not seem to be the sole explanation for the differences that we have found between the static batch adsorption performed on the Tecan Evo robot compared to results by batch adsorption presented by others [25,37].

In the light of the results presented above, we investigated the effect of incubation time on q_{max} and K_a. Hahn et al. incubated an unknown amount of MabSelect SuRe with IgG for 3 h [37], while we only incubated 7.7 μL for 2 h. Using a very simple setup with Eppendorph tubes, we incubated 7.7 μL resin with the same amount of IgG, varying only the incubation time. As seen from Fig. 11, our static adsorption experiment showed that the

Table 5
Interaction details from docking results. Arg^1 and Arg^2 are the first and second arginine from the N-terminal, respectively, for both ligands. Di-t-Bu-Phenol^2 and di-t-Bu-Phenol^3 are the phenol groups of D_2AAG in positions 2 and 3, respectively. MeOAc-NH is the protection group on the N-terminal, on which the ligand is coupled to the chromatographic support.

Amino acid		DAAG	D_2AAG
250	Thr	di-t-Bu-Phenol	–
251	Leu	di-t-Bu-Phenol	di-t-Bu-Phenol^3
252	Met	di-t-Bu-Phenol	di-t-Bu-Phenol^3
253	Ile	di-t-Bu-Phenol	di-t-Bu-Phenol^{2,3}
310	His	di-t-Bu-Phenol	di-t-Bu-Phenol^2
311	Gln	di-t-Bu-Phenol	di-t-Bu-Phenol^2
314	Leu	Arg^2	Arg^2
315	Asn	Arg^2	Arg^2
338	Lys	Arg^2	–
345	Glu	Arg^1	Arg^1
431	Ala	MeOAc-NH	Arg^1
432	Leu	Arg^1	Arg^1
433	His	Arg^1	Arg^1
434	Asn	di-t-Bu-Phenol	di-t-Bu-Phenol^3
435	His	di-t-Bu-Phenol	di-t-Bu-Phenol^3

maximum binding capacity was reached after 2 h; hence, incubation for longer periods does not affect the amount adsorbed significantly.

Our findings point to the fact that there are significant differences between the K_a values obtained by ITC using a free ligand and isotherms using ligands coupled to a base resin. Except for the small synthetic D_2AAG and DAAG ligands, we find that a free ligand/free protein setup such as ITC gives higher K_a values. Moreover, larger amounts of resin and longer incubation periods also seem to give increased K_a values obtained from batch adsorption experiments. These results may not be surprising; coupling of a ligand to a base resin may restrict the rotation of the ligand as well as limit the potential conformations compared to ITC. However, the difference is considerable when evaluating ligand performance and must be taken into account, e.g. if ITC is used for ligand selection.

3.6. Docking of peptide ligands to Fc fragment

We have discussed the differences in the results between D_2AAG and DAAG presented above by identification of a likely binding site on the Fc fragment. Fig. 12 shows representative docking modes for the two ligands DAAG and D_2AAAG with truncated linkers. The DAAG ligand scores considerably higher than the D_2AAG ligand; consequently, the DAAG ligand shows the best fit at the binding site where both ligands are most likely to interact with the Fc fragment. This result is well in line with our chromatographic and thermodynamic results; that the DAAG ligand binds IgG stronger and with a higher capacity compared to the D_2AAG ligand. As shown in Table 5, the two ligands may only differ in the interaction with Fc fragment amino acids Thr^{250}, Ile^{253}, Lys^{338} and Ala^{341}; hence, the variation in binding capacity and thermodynamic parameters may arise from these differences.

Ligand interaction appears to be a combination of a site specific pseudo affinity interaction as well as non-specific interaction. The strength of binding as well as the thermodynamic parameters is not influenced by the presence of the Fab-fragment. However, the apparent dependence of the binding stochiometry on the presence of the Fab-fragment may indicate that the binding site is in close proximity to the hinge region. Furthermore, the retention is mediated by hydrophobic interactions as well as through ionic interaction. The thermodynamic data indicates that the binding is primarily mediated by hydrophobic interactions since they are characterized by a numerically positive and favorable change in entropy. Ionic interactions are characterized by a numerically negative and hence unfavorable change in entropy. The thermodynamic data are well in line with the lack of IgG pI dependence of the binding capacity. However, the pH dependence on the binding of IgG also points to that ionic interactions are involved in the binding of IgG to the two small synthetic peptide ligands.

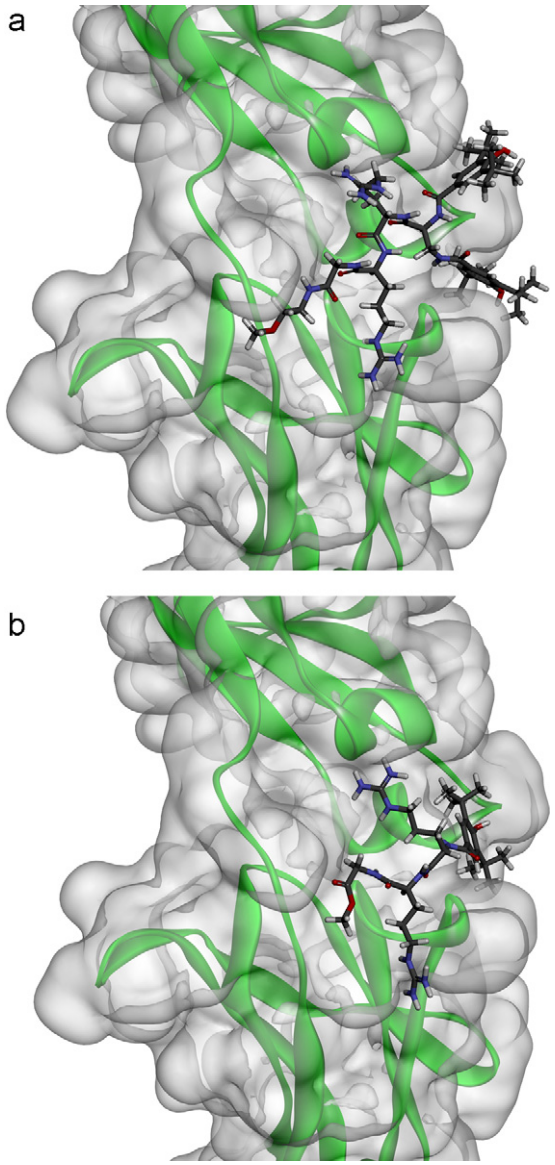

Fig. 12. Docking of D_2AAG (A) and DAAG (B) to Fc fragment. The backbone of the Fc fragment is shown as green ribbon, while the amino acid side-chains are depicted as a grey sphere. The ligands are shown as sticks, where blue represents nitrogen, light grey is hydrogen, dark grey is carbon and red is oxygen. (For interpretation of the references to color in this figure legend, the reader is referred to the web version of this article.)

4. Conclusion

We have presented two novel synthetic peptide ligands for IgG purification of which one in particular shows exciting results. Compared with commercial available IgG binding ligands such as MABsorbent A2P and MEP HyperCel, DAAG has a very high binding capacity of up to 48 mg/mL and with obtained mAb purities and recovery >90% when immobilized to the agarose based WorkBeads from Bio-Works. Moreover, the ligand has an association constant in the lower micromolar range and the interaction with the ligand

is entropically driven. Our results clearly show that the interaction with IgG is through the Fc fragment since $F(ab')_2$ fragments are not bound. Furthermore, the interaction between IgG and DAAG is influenced by the presence of $F(ab')_2$ as shown by the difference in binding stoichiometries between full length IgG and the Fc fragment, respectively. These results indicate that the binding site on the Fc fragment is located near the hinge region and hence, the presence of Fab on IgG only constitutes a steric hindrance to binding of more than one IgG molecule. In addition, our results show that the interaction is likely to be a combination of a specific interaction (pseudo-affinity) as well as non-specific interaction. It is likely that one ligand may interact specifically while adjacent ligand molecules interact in an non-specific manner as previously seen for PrtA. The interactions are hydrophobic as well as ionic.

Apart from purifying IgG from feedstock, the DAAG ligand may also be used for separating IgG aggregates in a subsequent polishing step after the initial purification and low pH treatment as a part of the virus clearance, potentially causing aggregate formation.

Our results show that the synthetic peptide ligand DAAG when coupled to WorkBeads shows promising results both as an alternative to a Protein A based capture step but also as a subsequent polishing step.

Acknowledgements

From Novo Nordisk A/S we would like to thank Dr. Anders Dybdal Nielsen for access to ITC equipment as well as Dr. Mathiass Wiendahl, Dr. Marcus Degermann and technician Mette Lund for assistance with the HTE setup and data analysis. Furthermore, we greatly appreciate the extensive work performed by technicians Signe Sørensen and Anja Hansen.

References

[1] S.R. Gallant, V. Koppaka, N. Zecherle, Methods Mol. Biol. 421 (2008) 61.
[2] Q.H. Shi, Z. Cheng, Y. Sun, J. Chromatogr. A 1216 (2009) 6081.
[3] A.C. Roque, G. Gupta, C.R. Lowe, Methods Mol. Biol. 310 (2005) 43.
[4] J.N. Carter-Franklin, C. Victa, P. McDonald, R. Fahrner, J. Chromatogr. A 1163 (2007) 105.
[5] M.A. Godfrey, P. Kwasowski, R. Clift, V. Marks, J. Immunol. Methods 160 (1993) 97.
[6] M.A. Godfrey, P. Kwasowski, R. Clift, V. Marks, J. Immunol. Methods 149 (1992) 21.
[7] D.S. Terman, Crit. Rev. Oncol. Hematol. 4 (1985) 103.
[8] D.K. Follman, R.L. Farner, J. Chromatogr. A 1024 (2004) 79.
[9] R. Wongchuphan, B.T. Tey, W.S. Tan, F.S. Taip, S.M.M. Kamal, T.C. Ling, Biochem. Eng. J. 45 (2011) 232.
[10] C.R. Lowe, S.J. Burton, N.P. Burton, W.K. Alderton, J.M. Pitts, J.A. Thomas, Trends Biotechnol. 10 (1992) 442.
[11] S.F. Teng, K. Sproule, A. Hussain, C.R. Lowe, J. Mol. Recognit. 12 (1999) 67.
[12] G. Fassina, A. Verdoliva, G. Palombo, M. Ruvo, G. Cassani, J. Mol. Recognit. 11 (1998) 128.
[13] P. Sinha, J. Sengupta, P.K. Ray, Biochem. Biophys. Res. Commun. 260 (1999) 111.
[14] B. D'Agostino, P. Bellofiore, M.T. De, C. Punzo, V. Rivieccio, A. Verdoliva, J. Immunol. Methods 333 (2008) 126.
[15] E. Boschetti, J. Biochem. Biophys. Methods 49 (2001) 361.
[16] S. Oscarsson, J. Porath, J. Chromatogr. 499 (1990) 235.
[17] H.O. Yang, P.V. Gurgel, R.G. Carbonell, J. Chromatogr. A 1216 (2009) 910.
[18] J. Chen, J. Tetrault, Y. Zhang, A. Wasserman, G. Conley, M. Dileo, E. Haimes, A.E. Nixon, A. Ley, J. Chromatogr. A 1217 (2010) 216.
[19] P. Gagnon, Curr. Pharm. Biotechnol. 10 (2009) 434.
[20] P. Gagnon, T. Arakawa, Curr. Pharm. Biotechnol. 10 (2009) 347.
[21] P. Gagnon, K. Beam, Curr. Pharm. Biotechnol. 10 (2009) 440.
[22] J. Chen, J. Tetrault, A. Ley, J. Chromatogr. A 1177 (2008) 272.
[23] A. Voitl, T. Muller-Spath, M. Morbidelli, J. Chromatogr. A 1217 (2010) 5753.
[24] P. Gagnon, N. Biotechnol. 25 (2009) 287.
[25] S. Ghose, B. Hubbard, S.M. Cramer, J. Chromatogr. A 1122 (2006) 144.
[26] S.F. Teng, K. Sproule, A. Husain, C.R. Lowe, J. Chromatogr. B: Biomed. Sci. Appl. 740 (2000) 1.
[27] J. Curling, Genet. Eng. News 21 (2001) 54.
[28] A.R. Newcombe, C. Cresswell, S. Davies, K. Watson, G. Harris, K. O'Donovan, R. Francis, J. Chromatogr. B: Anal. Technol. Biomed. Life Sci. 814 (2005) 209.
[29] S. Chhatre, N.J. Titchener-Hooker, A.R. Newcombe, E. Keshavarz-Moore, Nat. Protoc. 2 (2007) 1763.
[30] S.C. Burton, D.R. Harding, J. Chromatogr. A 814 (1998) 71.
[31] I. Johannsen, M.R.Galleco, R. Michael, D. Ambrosius, A. Jacobi, 2006. Patent no. WO 2006/066598, "Antibody Binding Affinity Ligands".
[32] G. Jones, P. Willett, R.C. Glen, A.R. Leach, R. Taylor, J. Mol. Biol. 267 (1997) 727.
[33] H.M. Berman, J. Westbrook, Z. Feng, G. Gilliland, T.N. Bhat, H. Weissig, I.N. Shindyalov, P.E. Bourne, Nucleic Acids Res. 28 (2000) 235.
[34] B.J. Horstmann, C.N. Kenney, H.A. Chase, J. Chromatogr. 361 (1986) 179.
[35] K. Wrzosek, M. Gramblicka, M. Polakovic, J. Chromatogr. A 1216 (2009) 5039.
[36] S. Ghose, B. Hubbard, S.M. Cramer, Biotechnol. Bioeng. 96 (2007) 768.
[37] R. Hahn, P. Bauerhansl, K. Shimahara, C. Wizniewski, A. Tscheliessnig, A. Jungbauer, J. Chromatogr. A 1093 (2005) 98.
[38] T. Bergander, K. Nilsson-Vaelimaa, K. Oberg, K.M. Lacki, Biotechnol. Prog. 24 (2008) 632.
[39] N. Tugcu, D.J. Roush, K.E. Goklen, Biotechnol. Bioeng. 99 (2008) 599.
[40] J.A. Queiroz, C.T. Tomaz, J.M. Cabral, J. Biotechnol. 87 (2001) 143.
[41] F.Y. Lin, C.S. Chen, W.Y. Chen, S. Yamamoto, J. Chromatogr. A 912 (2001) 281.
[42] M. Dieterle, T. Blaschke, H. Hasse, J. Chromatogr. A 1205 (2008) 1.
[43] J.J. Langone, C. Das, R. Mainwaring, W.T. Shearer, Mol. Cell. Biochem. 65 (1985) 159.
[44] L.N. Lund, T. Christensen, G. Houen, A. Staby, P.M. St. Hilaire, J. Mol. Rec. 24 (2011) 945.
[45] R. Hahn, R. Schlegel, A. Jungbauer, J. Chromatogr. B 790 (2003) 35.
[46] T. Herrmann, M. Schroder, J. Hubbuch, Biotechnol. Prog. 22 (2006) 914.